

Lawrence Berkeley National Laboratory

Recent Work

Title

THE SCINTILLATION CAMERA FOR RADIOISOTOPE LOCALIZATION

Permalink

<https://escholarship.org/uc/item/0jc9d66v>

Author

Anger, H.O.

Publication Date

1966-10-06

eg. 2

University of California

Ernest O. Lawrence Radiation Laboratory

THE SCINTILLATION CAMERA FOR RADIOISOTOPE LOCALIZATION

H. O. Anger

October 6, 1966

RECEIVED

LIBRARY AND DOCUMENTS DIV.

LIBRARY AND DOCUMENTS DIV.

TWO-WEEK LOAN COPY

This is a Library Circulating Copy
which may be borrowed for two weeks.
For a personal retention copy, call
Tech. Info. Division, Ext. 5545

UCRL-17284
eg. 2

DISCLAIMER

This document was prepared as an account of work sponsored by the United States Government. While this document is believed to contain correct information, neither the United States Government nor any agency thereof, nor the Regents of the University of California, nor any of their employees, makes any warranty, express or implied, or assumes any legal responsibility for the accuracy, completeness, or usefulness of any information, apparatus, product, or process disclosed, or represents that its use would not infringe privately owned rights. Reference herein to any specific commercial product, process, or service by its trade name, trademark, manufacturer, or otherwise, does not necessarily constitute or imply its endorsement, recommendation, or favoring by the United States Government or any agency thereof, or the Regents of the University of California. The views and opinions of authors expressed herein do not necessarily state or reflect those of the United States Government or any agency thereof or the Regents of the University of California.

Submitted to Journal of Nuclear Medicine

UCRL-17284
Preprint

UNIVERSITY OF CALIFORNIA

Lawrence Radiation Laboratory
Berkeley, California

AEC Contract No. W-7405-eng-48

THE SCINTILLATION CAMERA FOR RADIOISOTOPE LOCALIZATION

H. O. Anger

October 6, 1966

The Scintillation Camera for Radioisotope Localization*

H.O. Anger
Donner Laboratory of Medical Physics and Biophysics
and Lawrence Radiation Laboratory,
University of California,
Berkeley, Calif.

Ref.1

The first scintillation camera was built at Donner Laboratory 10 years ago. It employed a 4-inch diameter crystal viewed by seven phototubes, and was used clinically to take pictures of the thyroid gland with Iodine-131 (1). Although it gave satisfactory results, the small size of the crystal and other factors limited the resolution. Two years later, when larger crystals were available, an 8-inch camera was built, and it was used in 1958 to take the first time-lapse motion pictures of a dynamic process in vivo. The pictures were taken at the rate of one frame per minute after intravenous injection of 50 microcuries of I-131 Rose Bengal in a rat. They showed very rapid uptake of the dye in the liver, followed by excretion into the gut. Shown as motion pictures at the American Society of Nuclear Medicine meeting in 1960, they illustrated one of the principle advantages of radioisotope cameras over conventional scanners, namely that cameras can take pictures much more rapidly.

Fig.1

In 1961, when larger crystals became available, a camera with an 11-inch image detector was built. A cross section view of the image detector of this camera is shown in Fig.1. Near the bottom is the sodium iodide crystal, which is 11 inches in diameter and $\frac{1}{2}$ -inch thick, and a short distance above is the bank of 19 phototubes. When a gamma-ray interacts with the crystal, a scintillation consisting of 1000 to 5000 light photons is produced. This light divides among the phototubes in a manner depending on the location of the scintillation in the crystal. From the relative strengths of the output pulses, the electronic circuits determine the position of the scintillation.

* Based on a talk delivered at Gesellschaft für Nuklearmedizin E.V., Heidelberg, Oct. 6-8, 1966.

The brightness of the scintillation is determined by adding the pulses from all the phototubes, and this information is fed to a pulse-height selector. If the pulse-height requirements are met, the scintillation is displayed as a point flash of light in a cathode-ray tube. A time exposure is taken with a Polaroid camera, and after many thousands of dots are recorded, a picture of the subject results.

The overall resolving distance, or the distance apart of two point sources that are barely resolved as separate points by the camera, depends on two factors, the resolving distance of the particular collimator used, and the inherent resolving distance of the image detector. The inherent resolving distance of the image detector with the new bialkali phototubes is 6 mm for Iodine-131 and positron emitters and 9 mm for Technetium-99m (2, 3).

Ref.2,3

Gamma-Ray Camera

Four different collimators are used to image γ -ray emitters. In the Donner Laboratory camera they are mounted on a turret that can be rotated by hand to change collimators quickly and easily. The only important disadvantage of this arrangement is that the image detector cannot be tilted. It always points straight down, and lung or kidney pictures can not be taken with the patient in a sitting or standing position. The commercially available Nuclear-Chicago Pho/Gamma camera can be pointed in any direction, but more time is required to change collimators.

Fig.2

The four different collimators are shown in Fig.2. At the upper left is a single-aperture pinhole. In many ways this is the most versatile type of collimator. It gives the best combination of resolution and sensitivity for small subjects when they can be placed close to the aperture. It also provides the only method for taking single pictures of very large subjects at the present time. This is done simply by placing the subject a large distance from the aperture. The resolution and sensitivity decrease under these conditions, but it still gives useful results as shown later.

At the upper right is a triple-aperture pinhole collimator. This gives three simultaneous views of the thyroid gland - a conventional frontal view and two enlarged oblique views of the right and left lobes. In some cases, the three views show whether a nodule is anterior or posterior to the gland.

At the lower left is a multichannel collimator designed for use with medium-energy gamma-ray emitters, such as Iodine-131, Gold-198 and Mercury-203. It is 2.2 inches thick, has about 1600 holes, and gives the best combination of sensitivity and resolution for medium-sized subjects such as the brain and liver.

Fig.2

At the lower right of Fig.2 is a thin-septum multichannel collimator designed for use with low-energy gamma-ray emitters, such as Technetium-99m. This collimator has 4000 holes, and it gives about twice the sensitivity and better resolution than the medium-energy collimator.

The overall resolving distance R_o of the scintillation camera is given approximately by the equation, $R_o = (R_1^2 + R_c^2)^{1/2}$, where R_1 is the inherent resolving distance of the image detector alone, and R_c is the geometric resolving distance of the collimator (2). The geometric resolving distance R_c of the medium-energy multichannel collimator at a distance of 7.5 cm from the subject is about 14 mm. Since the inherent resolving distance of the image detector is 6 mm for Iodine-131, the overall resolving distance calculated from the above equation is about 15 mm for Iodine-131 at 3 inches. The scintillation camera delivers better resolution when the radioactive subject is closer to the collimator. At 1 cm distance the calculated overall resolving distance for Iodine-131 is about 9 mm.

Ref.2

The overall resolving distance of 15 mm at 3 inches is comparable to that delivered by scanners with coarse-focus collimators at their focal plane. However, the scintillation camera has better depth of field, or in other words it delivers good resolution over a wide range of distances between subject and collimator. Focused collimator scanners deliver their best resolution within a limited depth of field near their geometric focal plane. Therefore the camera is more satisfactory for imaging thick organs such as the liver.

Fig.3
Ref.3

The sensitivity of the scintillation camera to γ rays of various energies when using these collimators is shown in Fig.3 (3). Curve C gives the sensitivity with the medium-energy multichannel collimator. For the 0.36 MeV γ rays from Iodine-131, for example, it is 150 dots/minute/microcurie in air. Curve A gives the sensitivity with the low-energy multichannel collimator. For Technetium-99m, it is

about 900 dots/minute/microcurie in air. Curve B gives the sensitivity of the camera with ^{the} pinhole collimator close to the subject, as used for imaging the thyroid gland, and Curve D is the sensitivity when the subject is farther away from the same collimator, as it might be used for lung pictures. Point E at the top of the graph indicates the sensitivity of the positron camera, which is 2000 dots/minute/microcurie in air. The positron camera will be described later.

The figures quoted above are roughly 10 times the sensitivity obtained from conventional focused-collimator scanners when they scan the same areas.

The maximum counting rates permitted before overload of the electronic circuits occurs is up to 10^5 dots per second when γ -ray collimation is used. For positron coincidence operation, the rate is much lower as described later.

Phantom Studies

Fig.4

Pictures of a thyroid phantom taken with three different γ -ray collimators are shown in Fig.4. The phantom contained four microcuries of Mock Iodine-131 and was a true 3-dimensional representation of the thyroid gland. Picture no.1 was taken with a single 5 mm diameter pinhole, and it shows a frontal view of the gland with cold nodules at the upper right and lower left pole. Picture no.2 was taken with the triple-aperture pinhole, and it shows a frontal view in the center, and oblique views of each lobe at right and left. Picture no.3 was taken with the medium-energy multichannel collimator. Each exposure lasted 10 minutes.

Ref.2

The single pinhole collimator has the highest resolution under these conditions because it projects a magnified image of the thyroid gland onto the image detector. The inherent resolution of the image detector becomes a very minor factor in the overall resolution obtained, because $R_o = (R_c^2 + R_i^2/m^2)^{1/2}$ where m is the magnification factor (2). In the above example $m = 2.3$. The calculated overall resolving distance is about 7 mm when using a 5 mm diameter pinhole.

A special optical camera was used to record the images in several of the following examples. It has six lenses with progressively decreasing aperture sizes, and it records six small images simultaneously on one piece of Polaroid film. Polaroid film is very convenient to use because of its quick development, but it has a limited range of proper exposure. This problem is overcome by producing the six images with graded intensity. Proper density is obtained in at least one of the images, even if the exposure time or the amount of activity in the patient varies. There is no loss of information due to the characteristics of the film. In many cases, cold areas are shown best on one image, while hot areas are best seen on another. The observer selects whatever

image best shows the area he wants to examine. After becoming accustomed to the small size of the images, many people prefer them over larger pictures. It is quite easy to see the significant information in the small images when they are viewed at normal reading distance.

Fig.5

Scintiphotos of a phantom containing 25 μ c of Barium-133 are shown in Fig.5. This isotope has the same γ -ray energy as the principle γ ray from Iodine-131. Each set of six images was made with the six-lens camera described in the previous paragraph. The exposure time was 5 minutes, and 25 000 dots were recorded in each of the three examples.

Picture no.1 was taken with the phantom 1 cm from the collimator, no.2 was taken at 5 cm, and the third was taken at 10 cm. These pictures illustrate the moderate loss of resolution that occurs as the distance between collimator and subject increases. The phantom has 5 cold areas, only 4 of which can be seen here. The smallest visible cold spot is 1.5 cm in diameter, and the largest is 4 cm.

Fig.6

Scintiphotos of the same phantom filled with 370 micro-curies of Technetium-99m are shown in Fig.6. The low-energy multi-channel collimator was used, and the exposure time was only one minute. The smallest cold spot visible here is 1 cm in diameter. The improvement in resolution is due to a number of factors; the larger amount of activity, the higher sensitivity of the sodium iodide crystal to low-energy radiation, and the higher resolution of the collimator. These pictures are composed of about 250 000 dots.

Picture no.1 was taken with the phantom 1 cm from the collimator, and no.2 10 cm from the collimator. Picture no.3 was taken with 6.5 cm of water added to the space between the phantom and the collimator to show the slight additional loss of resolution due to scattering and absorption of the gamma rays.

The pulse-height selector helps to maintain resolution and contrast under this condition by eliminating most gamma rays scattered by the water.

Fig.7

Scintiphotos taken of a very large phantom representing the lungs with a single 6 mm diameter pinhole collimator are shown in Fig.7. The phantom contained 500 microcuries of Technetium-99m, and the exposure time was 2 minutes per picture. In picture no.1, the phantom was 30 cm from the aperture, and the diameter of field was about 40 centimeters. The phantom is 30 centimeters wide. Two cold areas are visible, the largest 5 centimeters in diameter and the smallest 2.5 centimeters in diameter. In picture no.2 the phantom was half as far, or 15 cm from the collimator. At this distance, not all of the phantom was in the field of view, but the resolution improves and three smaller cold spots, $1\frac{1}{2}$ centimeters in diameter, become barely visible. In picture no.3, the distance to the phantom is cut in half again and the same cold spots are very clearly shown.

This series of pictures shows the versatility of the pinhole collimator. It can be used to take all-inclusive pictures of very large areas, and then to take high-resolution pictures of smaller areas by moving closer. The pictures also illustrate that the sensitivity of a pinhole collimator is slightly lower around the edge of the field, as shown by the slight darker shading of the images at the edges. However, this effect is so small that it should not be a factor in clinical use, except where numerical data is to be obtained. The slight foreshortening, or magnification of the nearer parts of the subject, inherent in pinhole collimators is also a very minor disadvantage.

Positron Camera

Of the 92 chemical elements, not all have radioactive isotopes with half lives and gamma-ray emissions suitable for use in γ -ray cameras and scanners. But some of these elements have positron emitting isotopes. Examples are carbon, fluorine and iron. The positron camera, shown in Fig.8, is a sensitive instrument for imaging positron emitters (2). The subject is placed as close to the image detector as possible, and a focal detector is placed below. The focal detector consists either of a single scintillation counter, an array of counters as shown in Fig.8, or a large crystal viewed by an array of phototubes.

Fig.8

Ref.2

Fig.8

When a positron emitter decays, it always emits a pair of gamma rays that travel away from each other at 180° . When one gamma ray hits the focal detector, the other hits the image detector above the patient. Simultaneous counts in the two detectors actuate a coincidence circuit, and the scintillation in the image detector is displayed on the cathode-ray tube. Gamma-ray pairs leave the subject in random directions, and the image detector is flooded with gamma rays which have no simultaneous count in the focal detector. However, the coincidence circuit separates the correctly-oriented gamma rays from all the others, and the subject is imaged without the use of collimators.

There is a similarity between the formation of images in positron cameras and the formation of ordinary X-ray radiographs. In X-ray radiography, X-rays from the focal spot of the X-ray tube travel upward through the subject and hit the radiographic film. The image projected on the film is slightly enlarged.

In the positron camera, the radiation originates in the subject, but the geometry is similar. When a gamma-ray travels downward and hits the focal detector, the opposite gamma-ray travels

UCRL-17284

upward along the same straight line to hit the image detector. The focal detector is a focal point for all the gamma-ray pairs that form the image. The image projected on the image detector is slightly enlarged, just as in the case of X-ray radiographs.

Fig.5,6,9

The resolution of the positron camera is demonstrated in Fig.9. The same phantom used in Figs.5 and 6 was filled with $18\mu\text{c}$ of Gallium-68, a positron emitter with a 68-minute half life. The phantom was 7.5 cm from the image detector, and the exposure time was one minute for picture no.1 and 5 minutes for picture no.2. The 1 centimeter cold spot is visible in both cases.

Fig.10

The positron camera has a focal plane, or plane-of-best-resolution, that can be set electronically to any depth in the subject. The resolution obtained when a test source is placed at 4 different depths below the image detector is shown in Fig.10. On the left, the focal plane was set at 3 inches, and pictures were taken with the source at 1, 3, 5, and 7 inches. Excellent resolution is obtained at the 3-inch distance, but it falls off above and below.

On the right, the source was moved through the same depths as before, but in this case the focal plane was set to agree with the distance to the source. The resolution is excellent at all distances when this is done. By adding new electronic circuits to the positron camera, images of six different focal planes will be obtained simultaneously. Then, no matter how deep the activity is in the subject, one of the 6 images will show it with excellent resolution. This modification should be operating in the near future and will be tested under clinical conditions.

Positron coincidence cameras are characterized by high sensitivity in combination with high resolution, and the possibility of tomographic operation with simultaneous readout of several planes. The disadvantages, when compared to γ -ray cameras, are additional complexity and overload when more than about $50\mu\text{c}$ of

radioactivity is in close proximity to the image detector. This occurs because no collimator is employed, and high counting rates are produced by small amounts of activity. Only a small fraction of the counts in the image detector are coincident with counts in the focal detector and appear as dots in the image. Therefore, one to five minutes exposure time is usually required to accumulate a sufficient number of dots in the image. Fast dynamic studies can not be made with the positron coincidence camera in its present state of development.

When very large amounts of positron emitters are available, as when Oxygen-15, Carbon-11, and other short-half-life positron emitters are obtained from a cyclotron and when very short exposure times are required, a high-energy multichannel collimator should be employed, rather than the coincidence technique. Since millicurie amounts of radioactivity will be available, and since large amounts can be safely used because the radiation dose to the patient will be low as a result of the short half life, the high sensitivity of the positron coincidence camera will not be needed. The use of a high-energy multichannel collimator under these conditions should allow satisfactory images to be obtained with very short exposure times from positron emitters.

Clinical Examples

Fig.11

Frames from a motion picture film showing Technetium-99m going through a normal human heart and kidneys are reproduced in Fig.11. Ten millicuries was injected into the antecubital vein, and pictures were taken at the rate of one frame per second. The special low-energy multichannel collimator was used, and the camera viewed the patient's anterior chest. These pictures don't have the resolution of cineangiograms, but they show the speed of the γ -ray scintillation camera and its suitability for dynamic studies.

Ref.4

This type of heart study may have value as a screening procedure. It is easy to perform, and involves very little risk or inconvenience to the patient. This was done in collaboration with Dr. Alexander Gottschalk (4).

Ref.5

In the kidney series, the same procedure is followed except the camera is viewing the kidney region from the back. The first few frames show the isotope in the bottom of the lungs. Later, the aorta is visible, and then the kidneys become perfused with the isotope. Dr. Malcolm Powell has used this technique at Donner Laboratory to demonstrate kidney lesions in combination with Neohydrin Hg-203 and Hippuran I-131. All three isotopes are used in succession and pulse-height selection is employed to make the camera insensitive to the previously-used lower-energy isotopes (5).

Fig.12

The uptake of Fluorine-18, a reactor produced positron emitter with a 2-hour half life, in a patient with Paget's disease is shown in Fig.12. This patient received 280 μ c of F-18 in the form of sodium fluoride, and the pictures were taken 1-2 hours later with the positron coincidence camera. Each of the 11 circular

fields was exposed for 4 minutes. The extra pictures at right and left are less intense images obtained from the six-lens optical camera. This work was done in collaboration with Dr. Donald Van Dyke (6).

Ref.6

Other radioisotopes used in clinical diagnosis and research with the positron camera include Iron-52, an 8-hour, cyclotron-produced positron emitter which is used to image the distribution of erythropoietic bone marrow (7). The same isotope is being used to show the site of absorption of iron when ingested orally (8). Gallium-68, a 68-minute positron emitter obtained from a 270-day parent isotope, is used to locate brain tumors (9).

Ref.7

Ref.8

Ref.9

Lung Visualization

Fig.13

Preliminary results obtained from a new isotope with a 5-second half life that shows promise for visualizing the lung is shown in Fig.13. The new isotope is Iridium-191m, and its characteristics are as follows. The half life is 4.9 seconds, the gamma-ray energy is 0.129 MeV, which is slightly lower than Technetium-99, and the abundance of the gamma-ray is 20%. Eighty percent of the gamma-rays are internally converted to high speed electrons. The parent Osmium-191 has a half life of 16 days and is reactor-produced from natural Osmium by the reaction $Os^{190}(n,\gamma)Os^{191}$. The daughter comes off an ion exchange column in strong sodium chloride solution as the hexachloro-iridiate.

In this example the ion exchange column is connected by a short piece of tubing to a vein in the left hind leg of a dog. The daughter isotope flows through the femoral vein into the right side of the heart. Then it flows into the lung, and apparently diffuses into lung tissue, where it remains until it decays completely. Of course with a 5-second half life, complete decay occurs in less than a minute, so it is not necessary for the Iridium to remain in the lung very long. In this example, the isotope was infused continuously, and the pictures show the resulting steady-state condition. The exposure time for each circular field was 45 seconds. The two extra pictures at the left of the dog show the lung field at darker intensity.

In dogs, the heart is superimposed on the lung, but in humans most of the lung is clear of the heart, so this technique may be useful for visualizing the lung in humans. Compared to other agents for visualizing the lung, this method has the advantage of no particles to clog capillaries and very low radiation dose. This work has been done in collaboration with Mr. Yukio Yano, chemist at Donner Laboratory (10). This technique of con-

tinuous infusion of an isotope, followed by temporary uptake in an organ, and then followed by swift decay of the isotope within the organ, may be useful in other instances.

Transverse Section Views

Ref.11 The next four figures show work in progress by which
 transverse section scans of the brain, similar to those obtained
 with a special tomographic scanner by Kuhl (11), will be obtained
 with the γ -ray scintillation camera and auxiliary equipment. The
 patient will sit in a chair which rotates slowly about its
Fig.14 vertical axis as shown in Fig.14. The Nuclear-Chicago scintilla-
 tion camera will be used with a special collimator which is
 focused in one axis, as seen in the bottom drawing, but un-
 focused, or parallel, in the other axis, as seen in the top
 drawing. During rotation of the patient, the camera will examine
 a horizontal slice of tissue through the patient's head.

Fig.15 The optical camera that records the pictures will be
 special to two ways, as shown in Fig.15. First an array of glass
 rods will be located in front of the lens. This will transform
 the dots on the oscilloscope to vertical lines on the film. Second-
 ly, the film will be rotated about its perpendicular axis in
 synchronism with the patient. As the radioactive subject and the
 photographic film rotate in synchronism, a large number of lines
 will be recorded on the film that intersect wherever a radioactive
 point exists in the subject. The result will be the same as that
 obtained from a transverse body-section scanner when it makes a
 large number of linear scans around the patient's head and records
 the counting information as lines, according to the method of Kuhl.

Fig.16,17 Figures 16 and 17 show how this idea has been tested so
 far. Three small sources of Iodine-131 were fastened to a wheel,
 and the wheel was rotated through 24 different positions, stopping
 for a short exposure of the film every 15°. The wheel was viewed
 from its edge at all times.

Fig.17 The result is seen in Fig.17. Picture no.1 shows a con-
 ventional image of the test sources, with the wheel in only one
 of the 24 positions. All three sources are visible, but it is

not possible to determine their depth below the collimator from this picture alone. Picture no.2 shows the same situation, except the glass rod filter was placed in front of the optical camera lens. The dots have been transformed into vertical lines.

Picture no.3 shows the result when the film and the wheel holding the sources have been rotated through 24 positions. The lines intersect at three locations corresponding to the location of the three sources. A transverse view has been produced that shows the location of the sources as viewed from right angles to the scintillation camera. Because of the mechanical simplicity of this system compared to transverse section scanners, it should have important applications in the diagnosis of brain tumors. Clinical trials will be made in the near future.

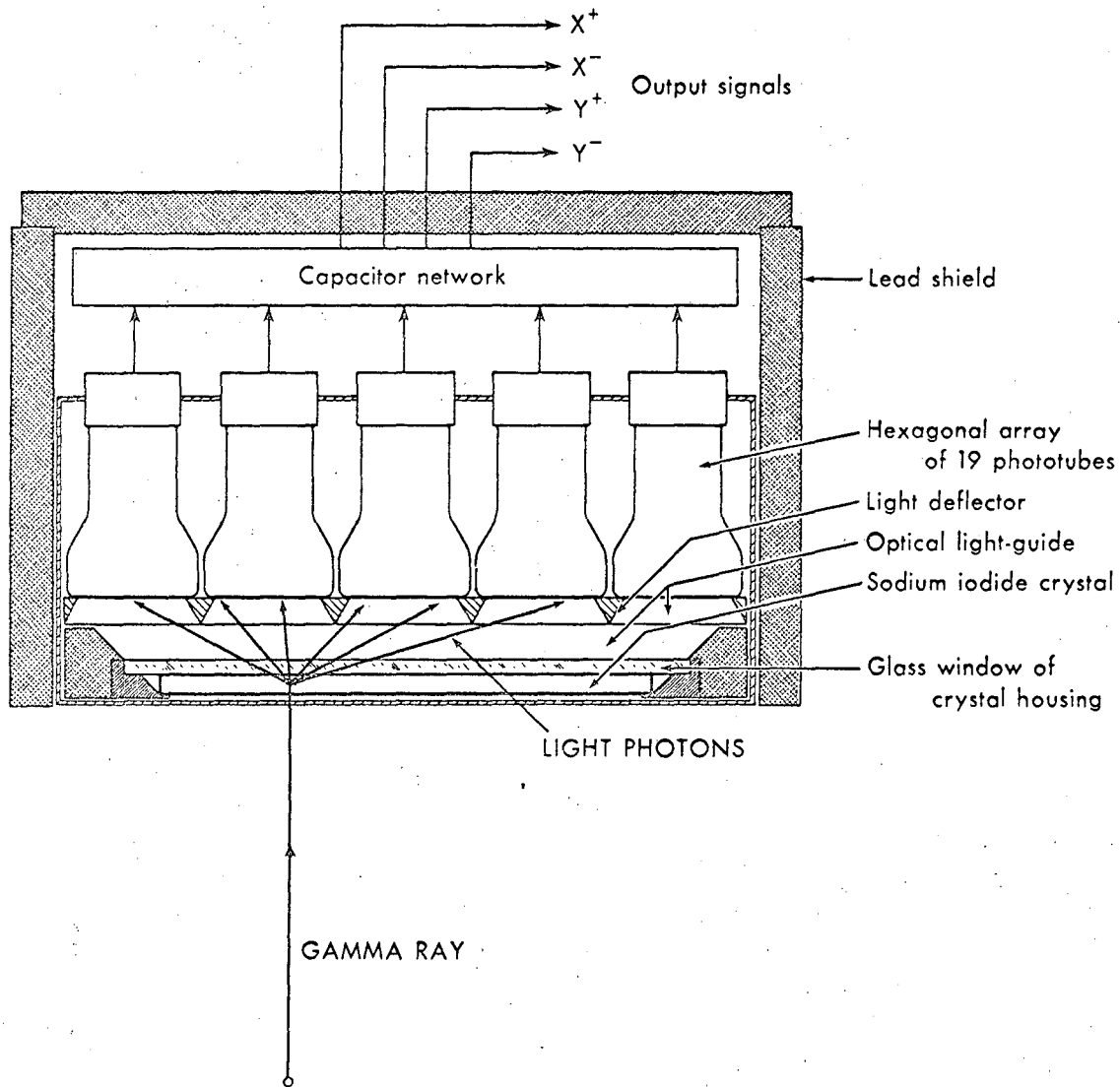
References

1. H.O. Anger, Rev. Sci. Inst. 29, 27 (1958).
2. H.O. Anger, in "Instrumentation in Nuclear Medicine", Ed. Gerald J. Hine, Academic Press, New York (to be published 1966).
3. H.O. Anger, Lawrence Radiation Laboratory Report UCRL-16724 (1966).
4. H.O. Anger, D.C. Van Dyke, A. Gottschalk, Y. Yano, and L.R. Schaer, Nuclonics 23, No.1, 57 (1965).
5. H.O. Anger, M.R. Powell, D.C. Van Dyke, L.R. Schaer, R. Farwas, and Y. Yano, ~~Recent Applications of the Scintillation Camera~~, in "Radioaktive Isotope in Klinik und Forschung", K. Fellingner and R. Höfer, Ed., Vol.7, Urban and Schwarzenberg, Munich and Berlin (1960).
6. D.C. Van Dyke, H.O. Anger, Y. Yano, and C. Bozzini, Am. J. Physiol. 209, 65 (1965).
7. H.O. Anger, and D.C. Van Dyke, Science 144, 1587 (1964).
8. R.A. Fawwaz, H.S. Winchell, M. Pollycove, T. Sargent, H. Anger, and J.H. Lawrence, J. Nucl. Med. 7, 569 (1966).
9. A. Gottschalk, K.R. McCormack, J.E. Adams, and H.O. Anger, Radiology 84, 502 (1965).
10. Y. Yano, and H.O. Anger, Use of Ultra-Short-Lived Radioisotopes to Visualize Blood Vessels and Lungs, (to be published).
11. D.E. Kuhl, in "Medical Radioisotope Scanning", Vol.I, International Atomic Energy Agency, Vienna (1964).

Figure Captions

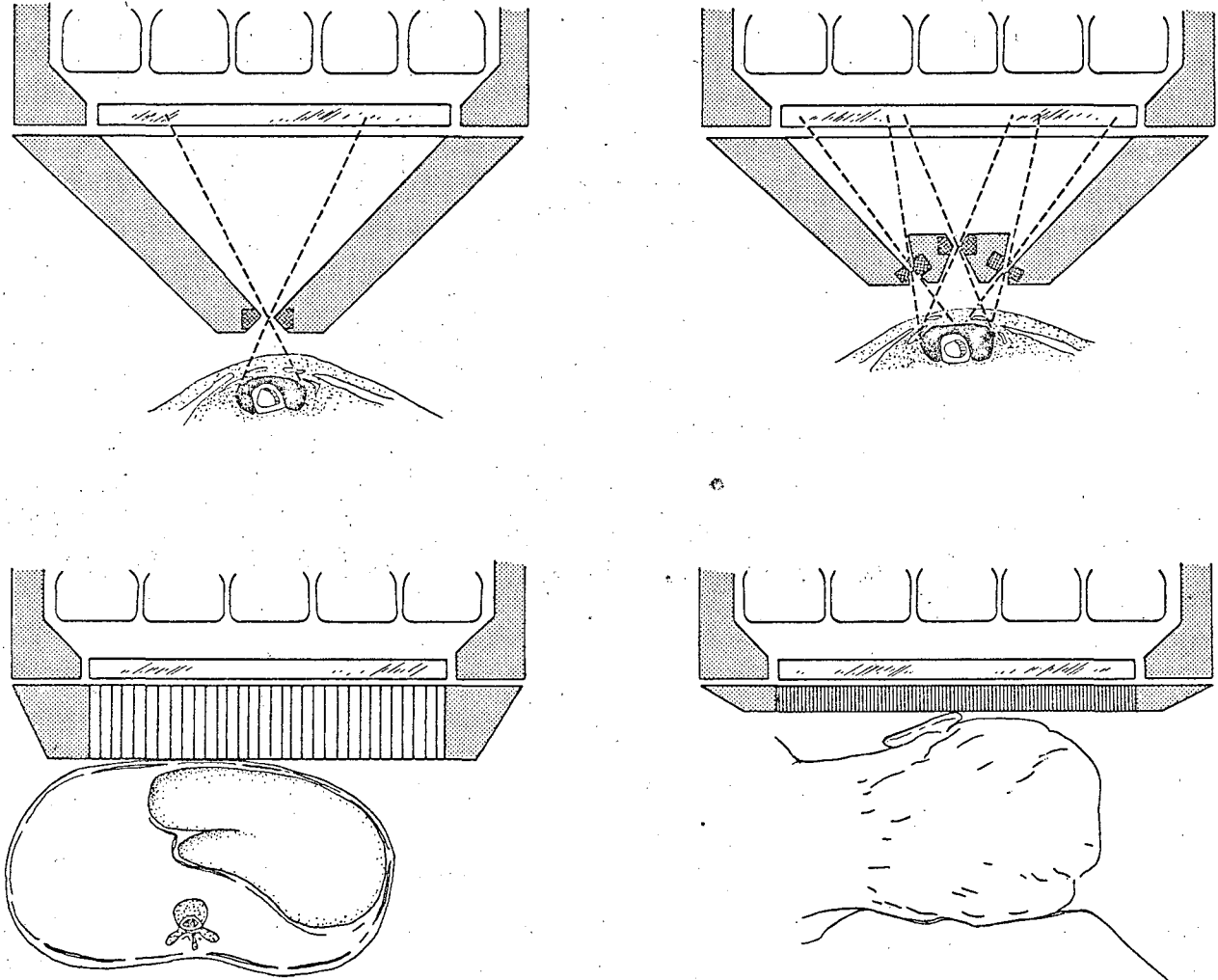
1. Image detector of scintillation camera with 11.5-inch diameter by 0.5-inch thick solid sodium iodide crystal and 19 multiplier phototubes.
2. Image-producing γ -ray collimators used with image detector of Fig.1.
3. Sensitivity of scintillation camera with three collimators shown in Fig.2, and in positron coincidence operation.
4. Scintiphotos of thyroid phantom obtained with (1) Single-aperture pinhole, (2) Triple-aperture pinhole, and (3) Medium-energy multichannel collimator.
5. Phantom containing 25 microcuries of Barium-133 imaged with medium-energy multichannel collimator, (1) Phantom 1 cm, (2) 5 cm, and (3) 10 cm from collimator. Exposure time 5 minutes. Six-lens optical camera was used to obtain six images of graded intensity simultaneously.
6. Phantom containing 370 microcuries of Technetium-99m imaged with low-energy multichannel collimator. Distance from phantom to collimator is (1) 1 cm, (2) 10 cm, and (3) 10 cm including 6.5 cm water. Exposure time 1 minute.
7. Lung phantom containing 500 microcuries Technetium-99m imaged with 6 mm pinhole collimator. Distance from phantom to aperture is (1) 30 cm, (2) 15 cm, and (3) 7.5 cm. Exposure time 2 minutes.
8. Block diagram of positron coincidence camera.
9. Phantom containing 18 microcuries of positron-emitting Gallium-68 imaged by positron coincidence technique. Exposure times (1) 1 minute and (2) 5 minutes. Phantom was 7.5 cm from image detector.
10. Resolution of positron coincidence camera (Left) with focal plane set at 3 inches and (Right) with focal plane set to source plane.
11. Dynamic function study of normal heart and kidneys made with Technetium-99m pertechnetate.
12. Uptake of Flucrine-18 in patient with Paget's disease.

13. Visualization of lung with 5-second Iridium-191m. Isotope is introduced into vein in right hind leg of dog, flows through veins and heart into lung where it diffuses into lung tissue. Isotope decays before leaving lung.
14. Planned use of scintillation camera to obtain transverse section images of brain.
15. Special optical camera for obtaining transverse section views. Array of glass rods before lens transforms dots into lines on photographic film.
16. Array of test sources on rotating wheel to demonstrate transverse section operation shown in Fig.17.
17. (1) Conventional scintiphoto of test sources shown in Fig.16. (2) Same except dots have been transformed into lines by glass rod filter shown in Fig.15. (3) Same except wheel holding sources and photographic film have been rotated through 24 positions, resulting in a transverse section view. This principle will be applied to brain tumor localization.



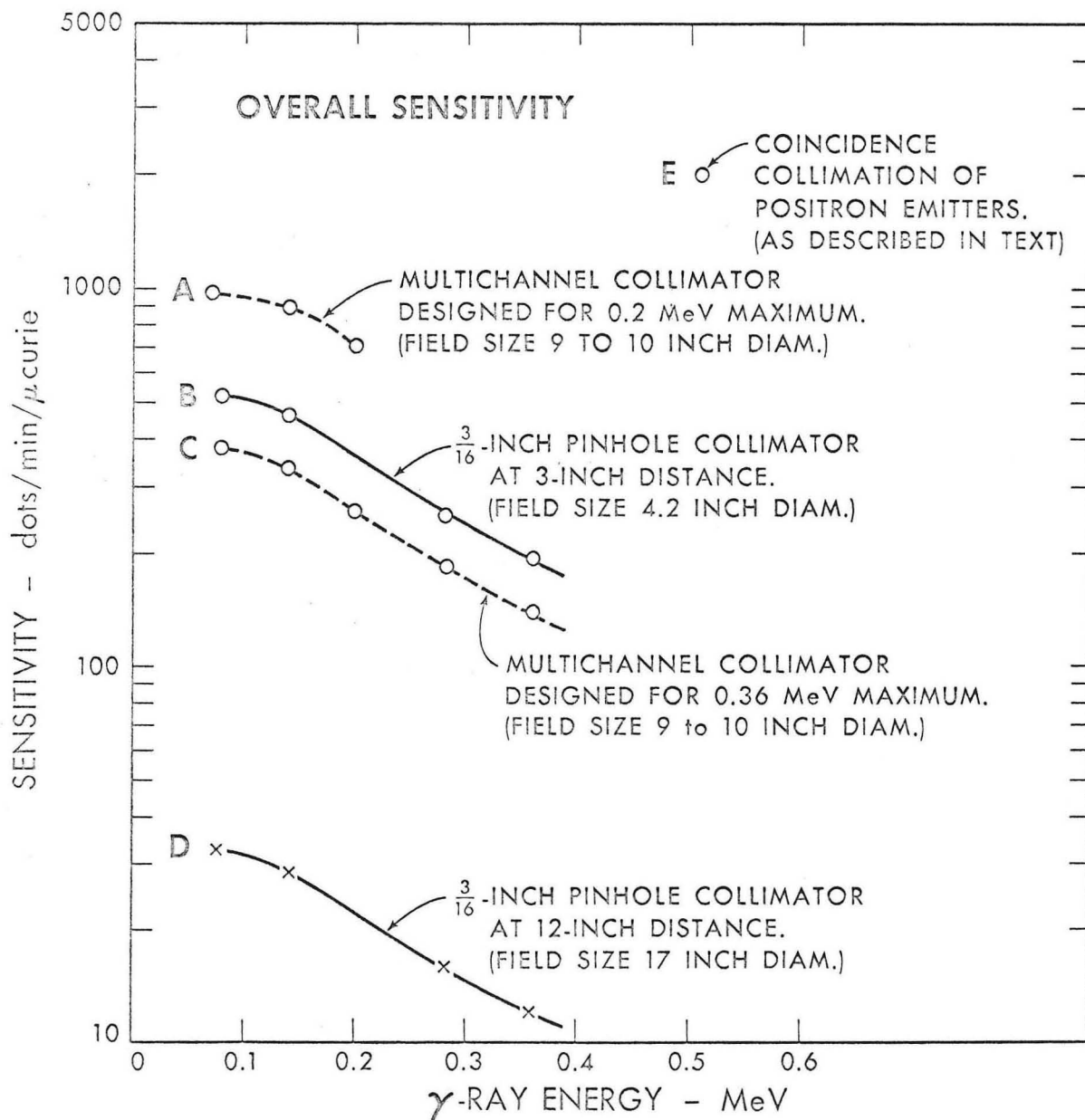
MUB-9644

Fig. 1



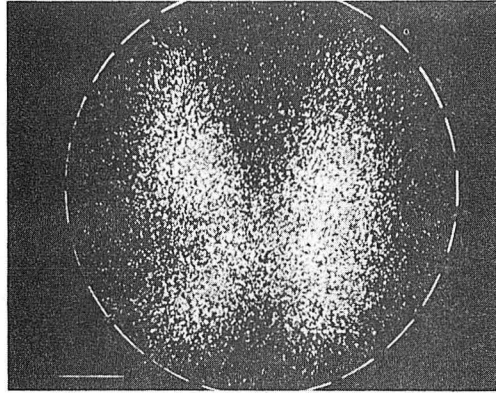
MUB-3834

Fig. 2

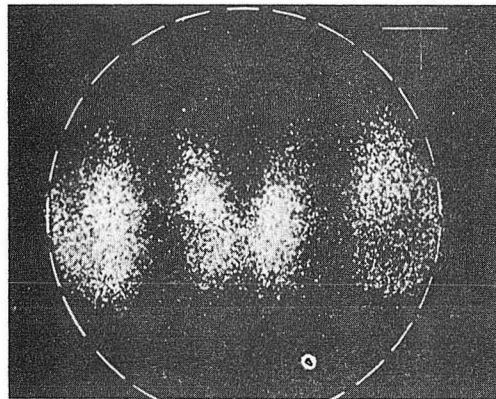


MUB - 9838

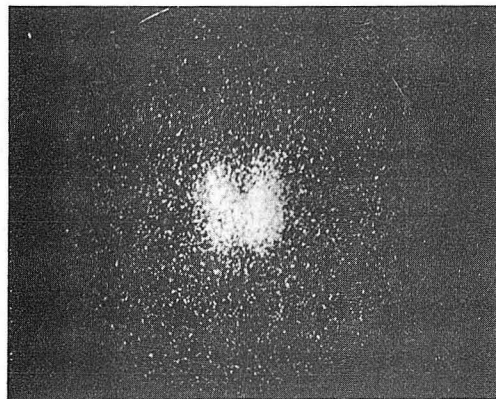
Fig. 3



(1)



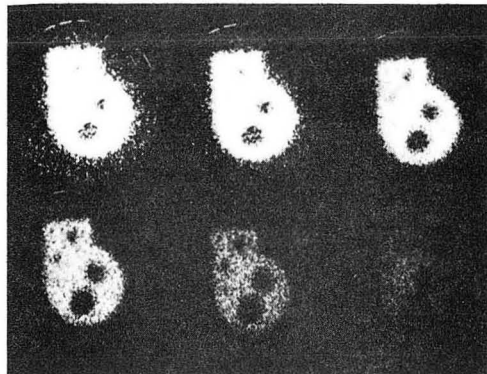
(2)



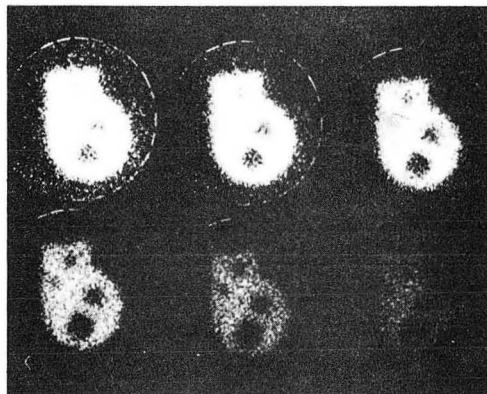
(3)

XBB 674-2288

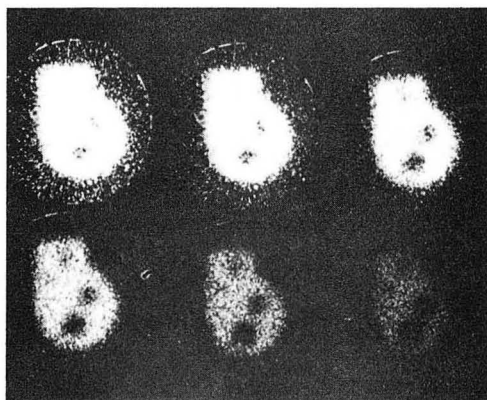
Fig. 4



(1)



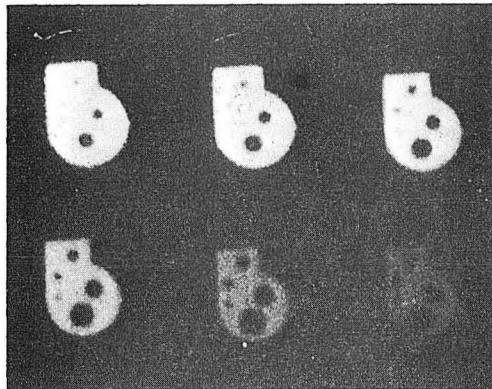
(2)



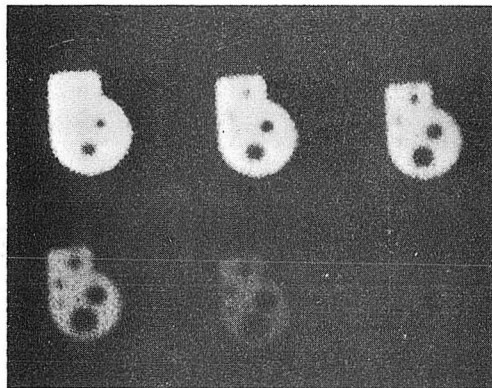
(3)

XBB 674-2289

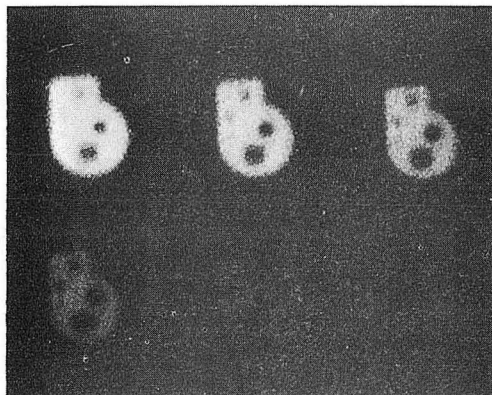
Fig. 5



(1)



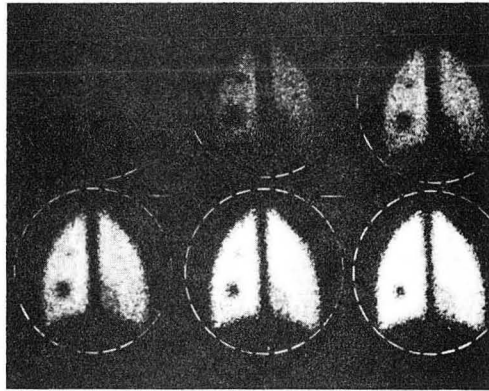
(2)



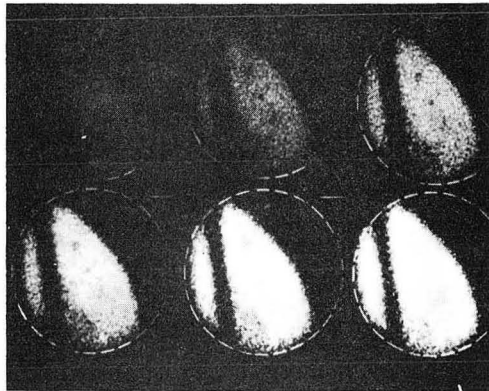
(3)

XBB 674-2290

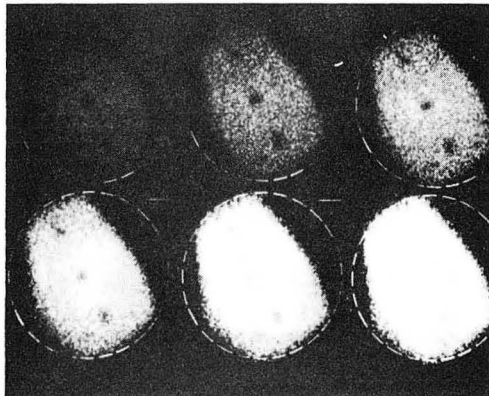
Fig. 6



(1)



(2)



(3)

XBB 674-2291

Fig. 7

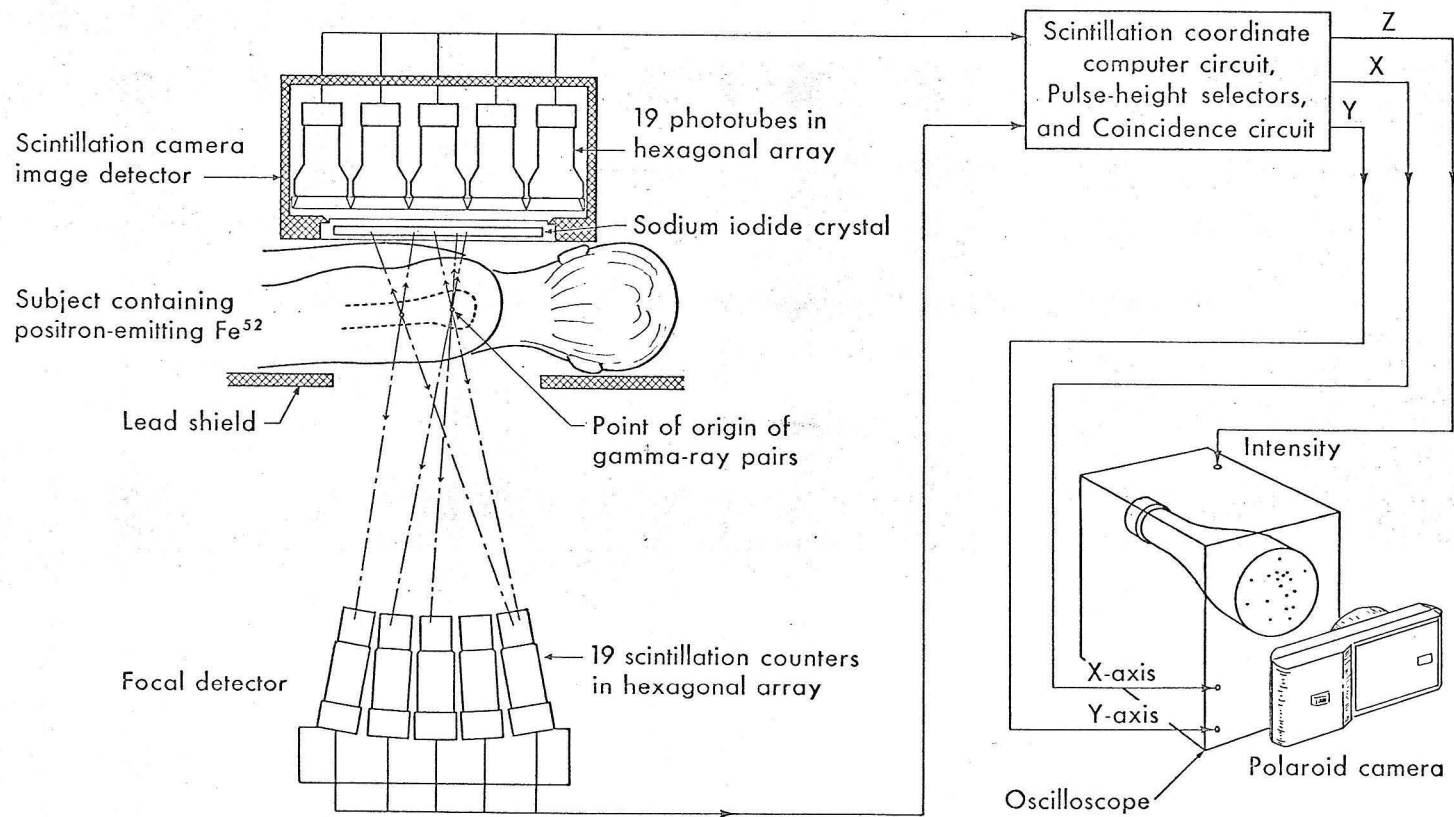
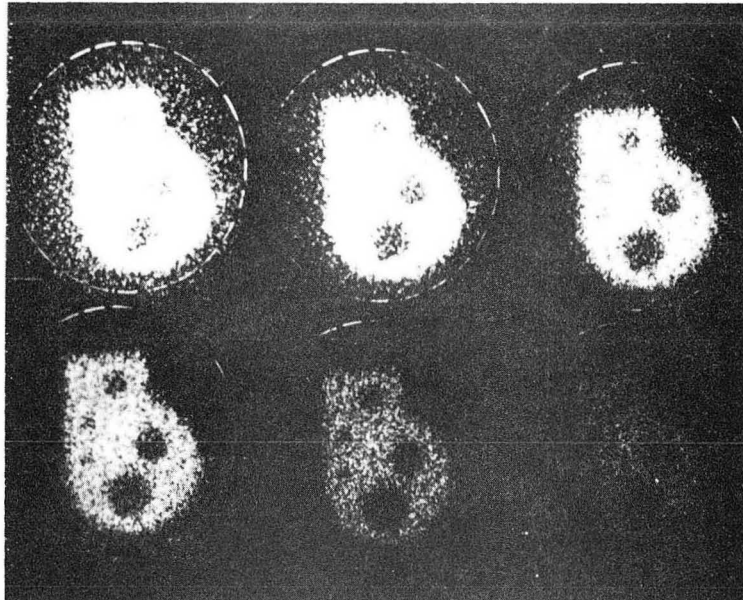
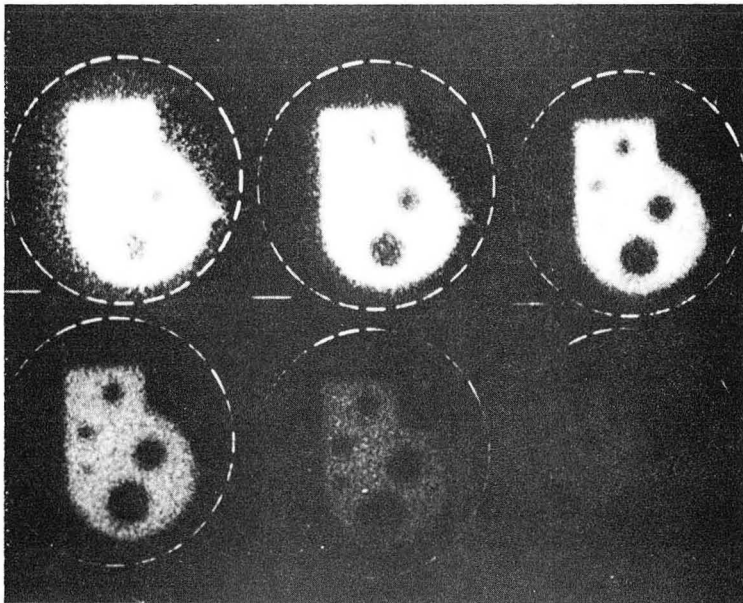


Fig. 8

MUB-2473



(1)



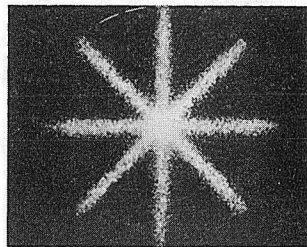
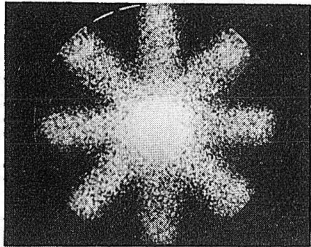
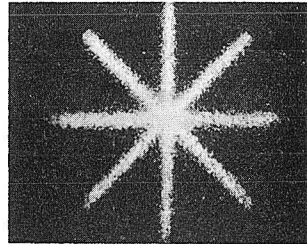
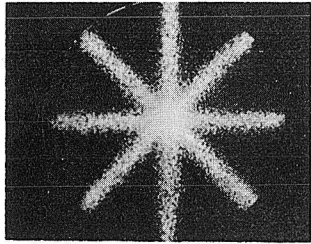
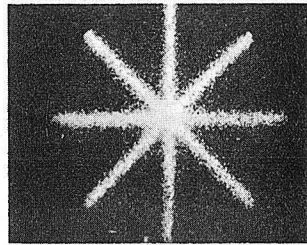
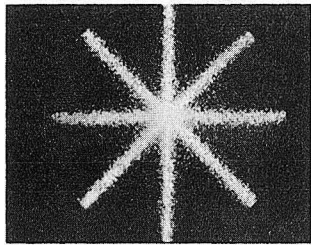
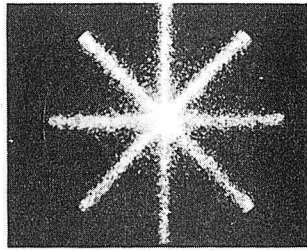
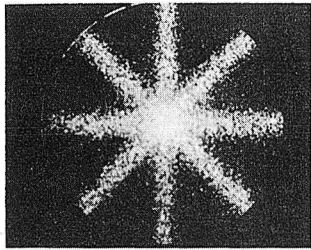
(2)

XBB 674-2292

Fig. 9

FOCAL PLANE FIXED
AT 3 INCHES

FOCAL PLANE SET
TO SOURCE PLANE



1"

3"

5"

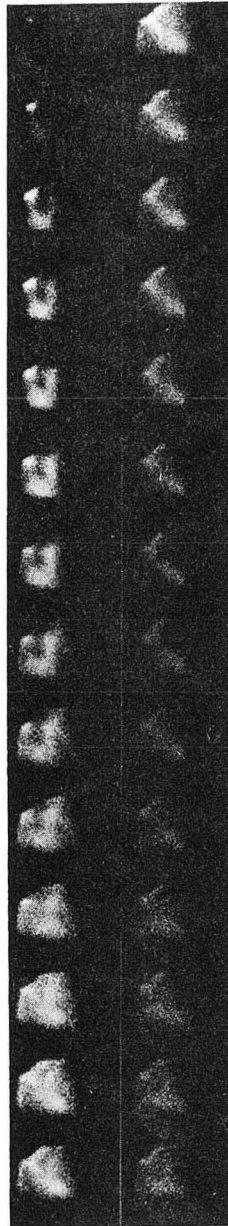
7"

DISTANCE
FROM
IMAGE
DETECTOR
TO
SOURCE
PLANE

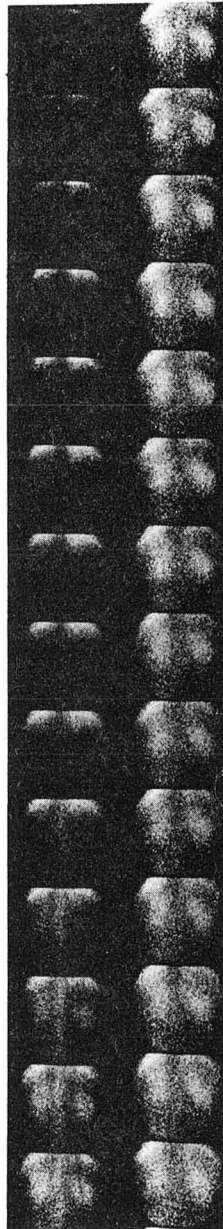
ZN-5412

Fig. 10

HEART
Tc^{99m}
**1 sec/
frame**

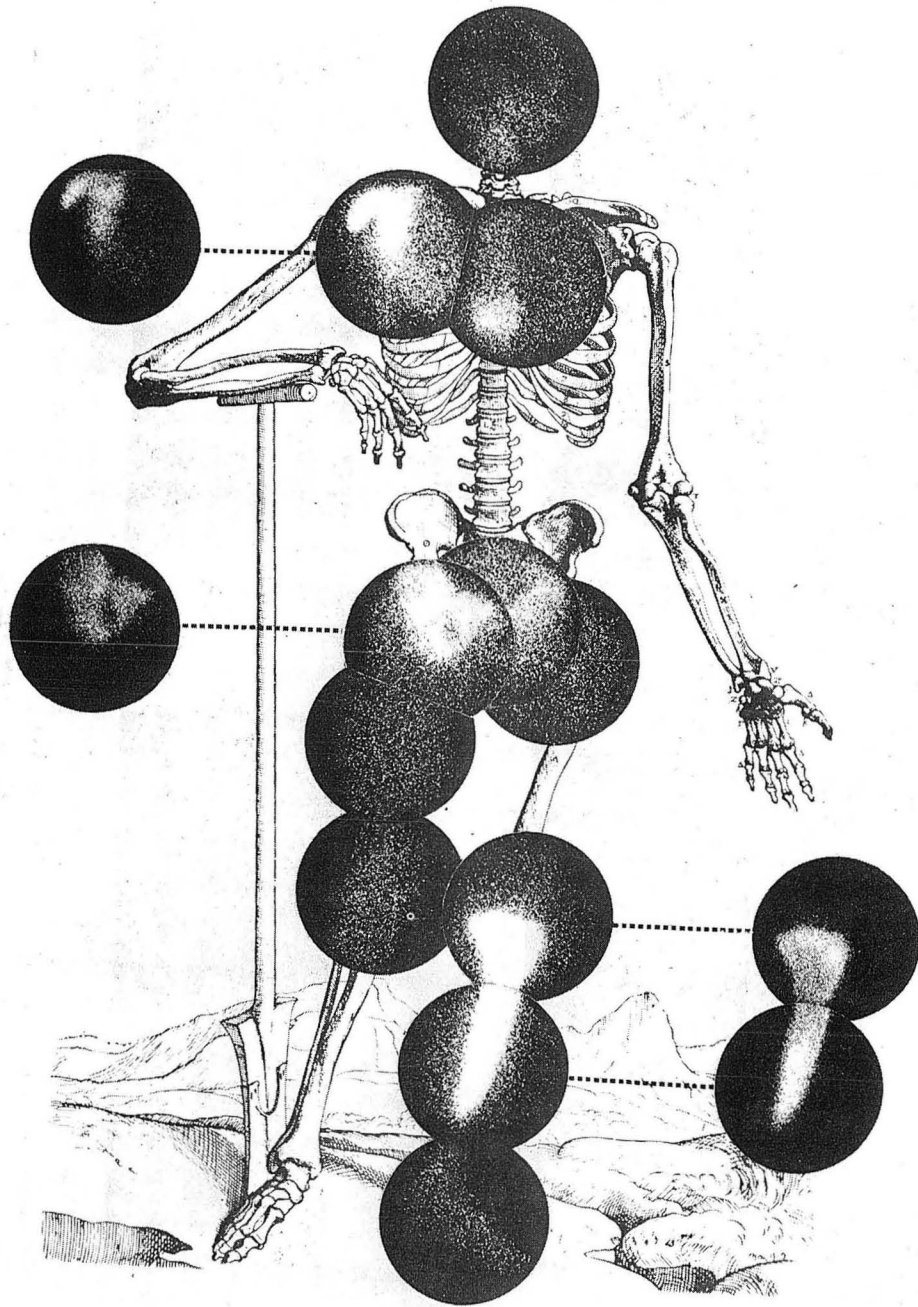


KIDNEY
Tc^{99m}
**1 sec/
frame**



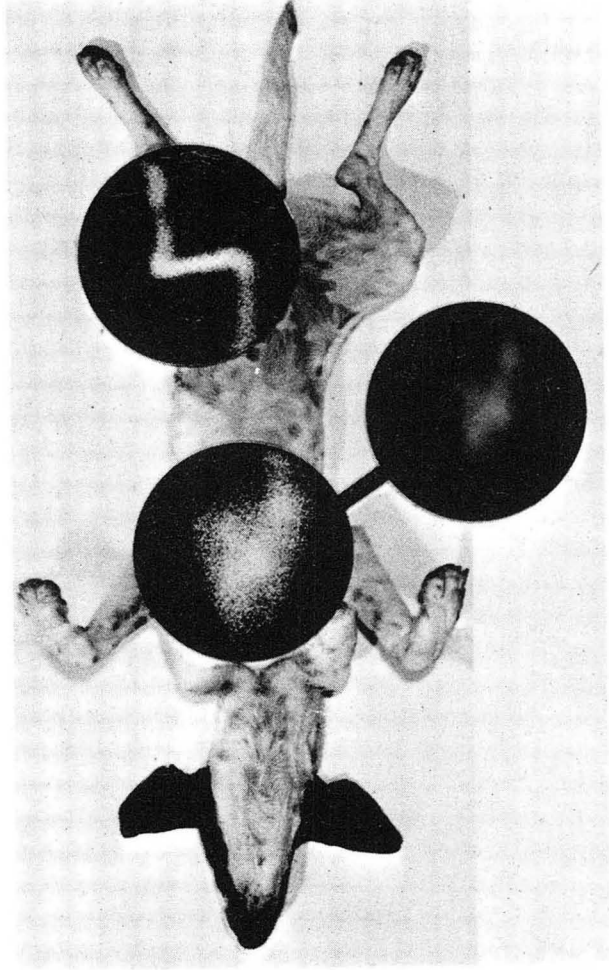
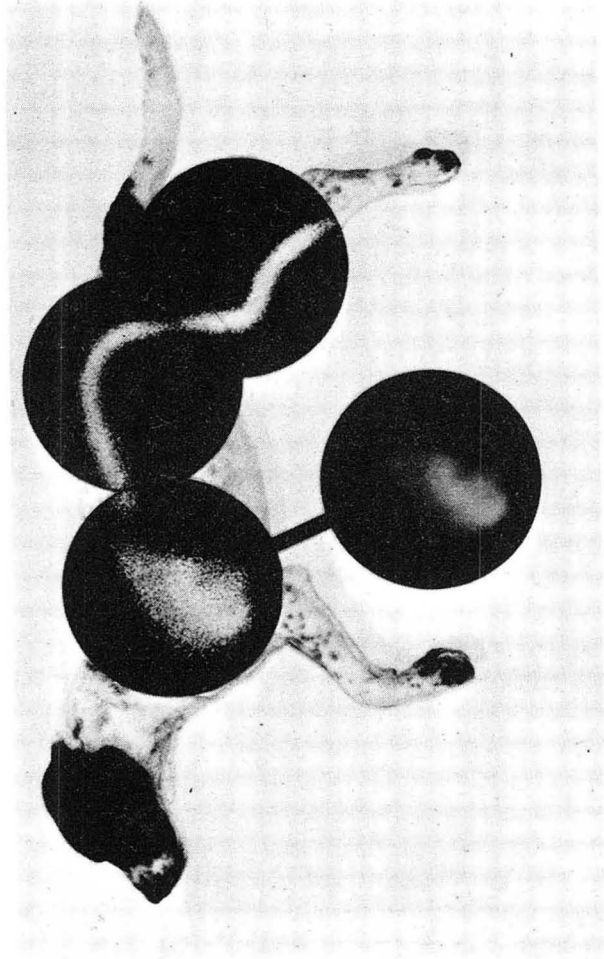
ZN-5414

Fig. 11



JHL 5993

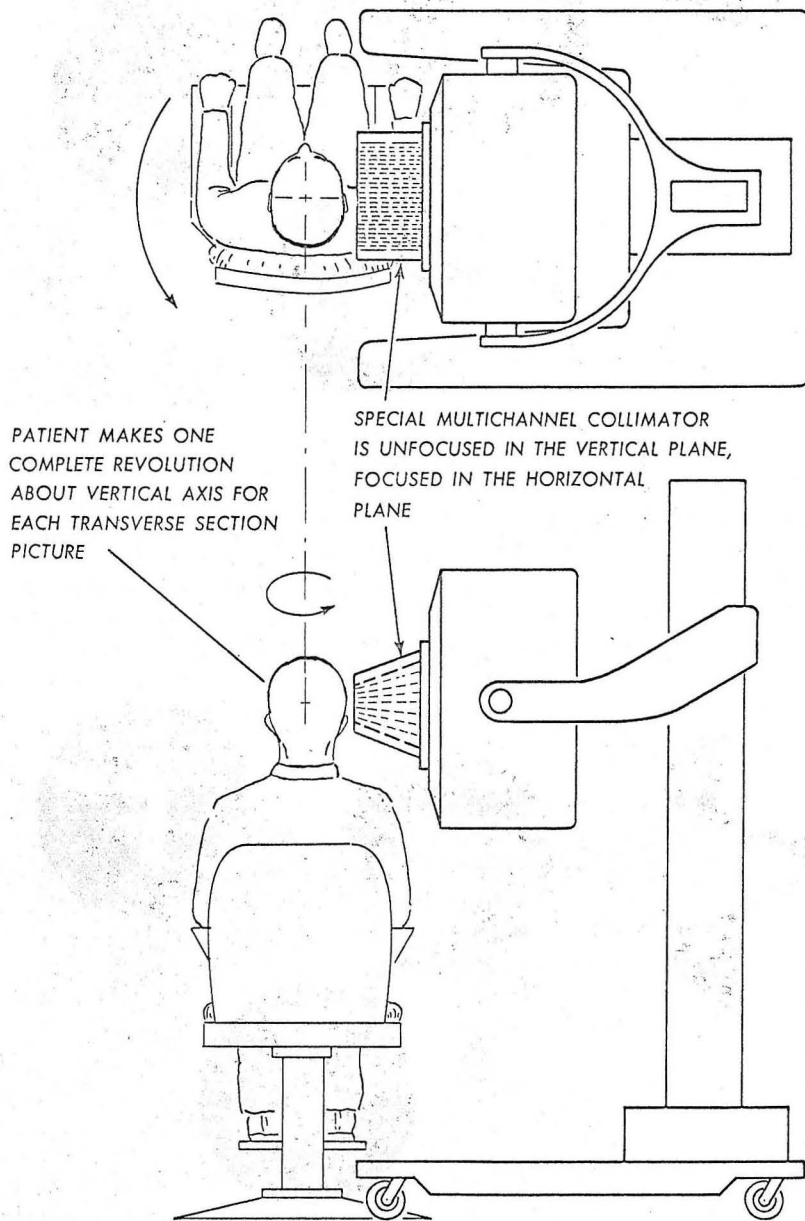
Fig. 12



ZN-5976

Fig. 13

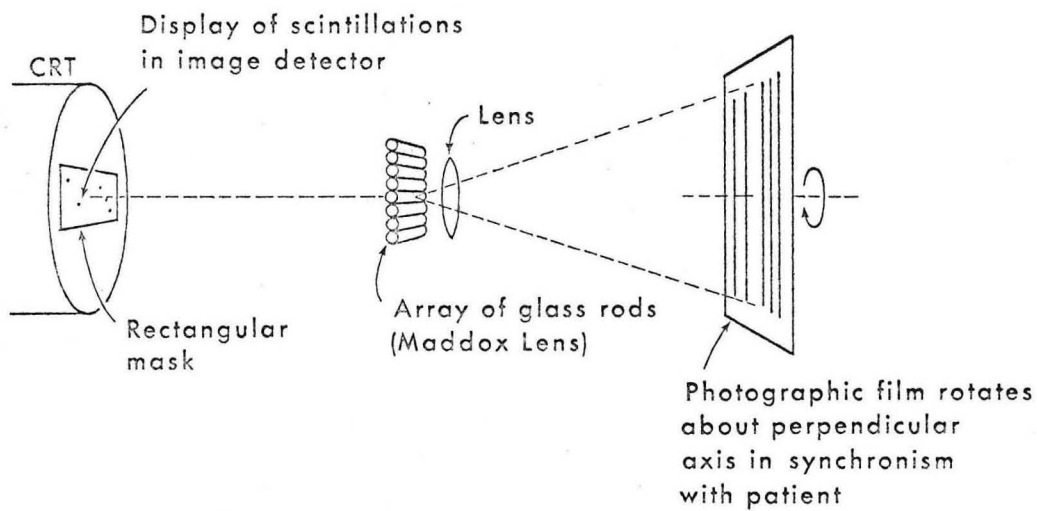
USE OF SCINTILLATION CAMERA FOR TRANSVERSE-SECTION VIEW OF BRAIN



MUB-12371

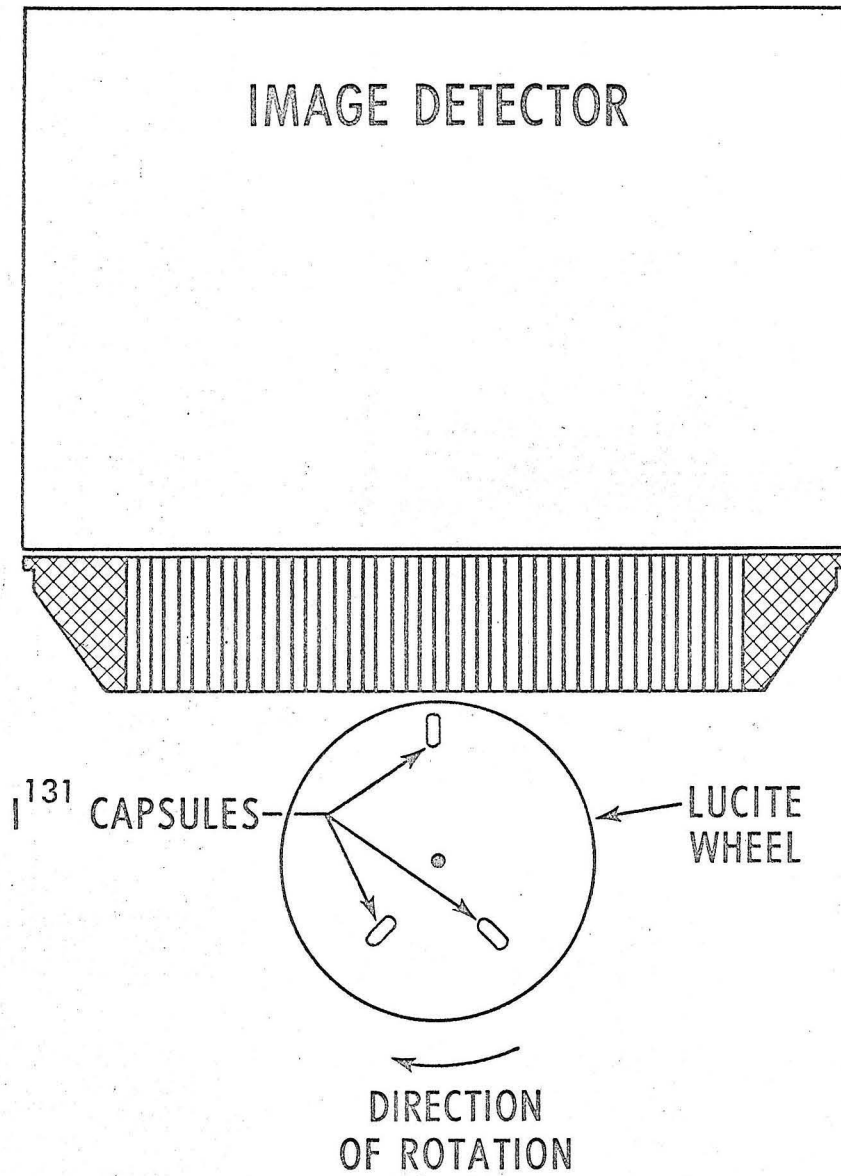
Fig. 14

TRANSVERSE BODY-SECTION ^SOCILLOSCOPE CAMERA



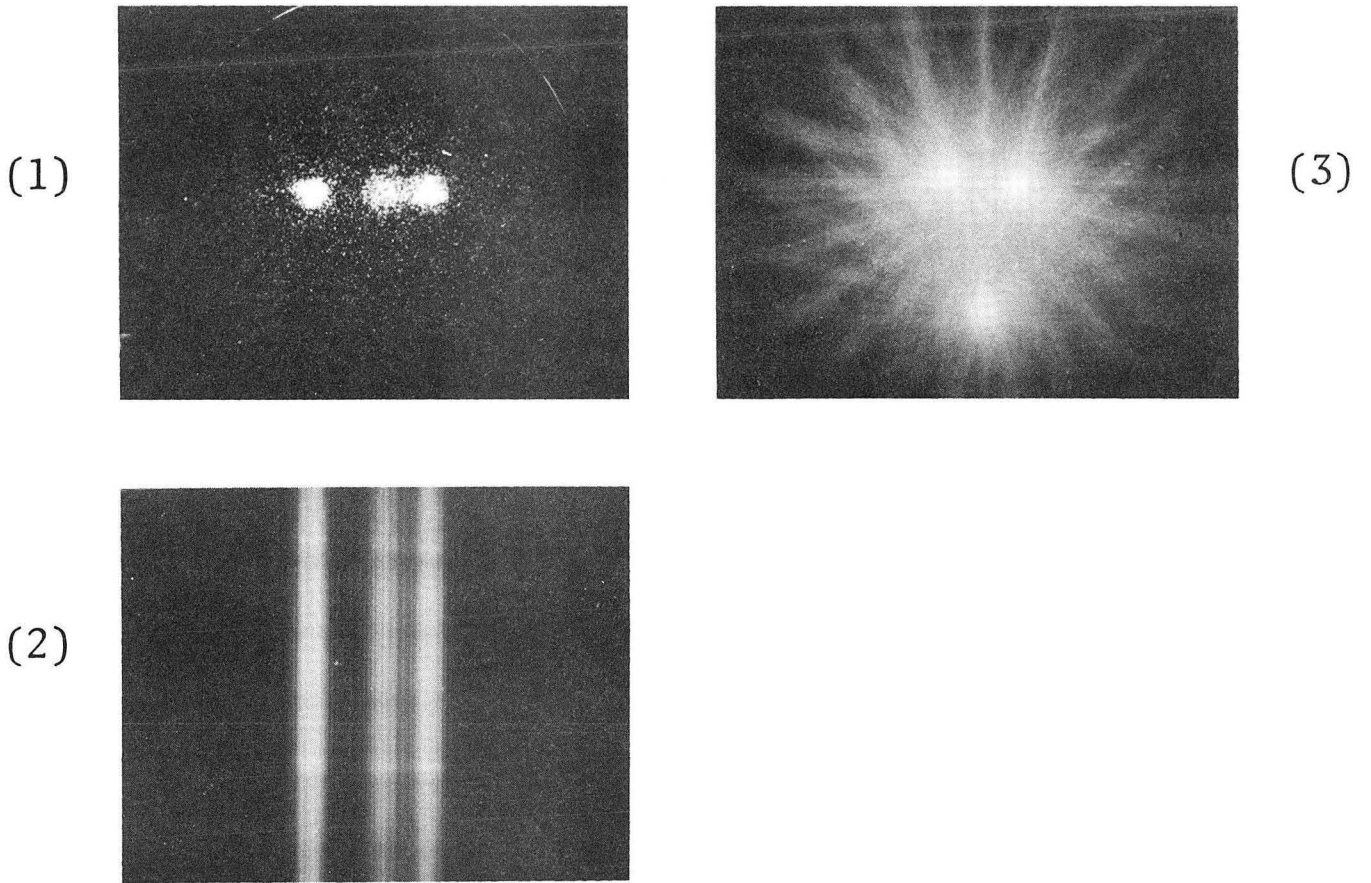
MUB-12580

Fig. 15



MUB-12835

Fig. 16



XBB 674-2293

Fig. 17

This report was prepared as an account of Government sponsored work. Neither the United States, nor the Commission, nor any person acting on behalf of the Commission:

- A. Makes any warranty or representation, expressed or implied, with respect to the accuracy, completeness, or usefulness of the information contained in this report, or that the use of any information, apparatus, method, or process disclosed in this report may not infringe privately owned rights; or
- B. Assumes any liabilities with respect to the use of, or for damages resulting from the use of any information, apparatus, method, or process disclosed in this report.

As used in the above, "person acting on behalf of the Commission" includes any employee or contractor of the Commission, or employee of such contractor, to the extent that such employee or contractor of the Commission, or employee of such contractor prepares, disseminates, or provides access to, any information pursuant to his employment or contract with the Commission, or his employment with such contractor.

